Dynamical memory underlies prolonged plasmid persistence after transient antibiotic treatment

Zhengqing Zhou[1,2,*], Andrea Weiss[1,2,*], Zhixiang Yao[1,2,6], Xiaoli Chen[1,2], Kristen Lok[1,2], Hye-in Son[1,2], Lingchong You[1,2,3,4,5,+]

1 Department of Biomedical Engineering, Duke University, Durham, North Carolina, USA

2 Center for Quantitative Biodesign, Duke University, Durham, North Carolina, USA

3 Center for Biomolecular and Tissue Engineering, Duke University, Durham, North Carolina, USA

4 Center for Genomic and Computational Biology, Duke University, Durham, North Carolina, USA

5 Department of Molecular Genetics and Microbiology, Duke University School of Medicine, Durham, North Carolina, USA

6 Present address: Innovative Genomics Institute, University of California, Berkeley, California, USA

*These authors contribute equally to the work.

[+]Correspondence and requests for materials should be addressed to Lingchong You. E-mail: lingchong.you@duke.edu; Tel: 919-660-8408; Fax: 919-668-0795.

Abstract

Plasmids play critical roles in spreading and maintaining antimicrobial resistance (AMR). They often exhibit prolonged persistence upon antibiotic treatment, even when they impose substantial burden on their hosts. This persistence has been primarily attributed to rapid horizontal transfer or low plasmid cost. However, these mechanisms cannot account for the slow decay of non-mobilizable, burdensome plasmids. Here, we show that the decoupling of time scales between slow segregation loss and fast growth competition leads to a slow-down in plasmid abundance decay at high plasmid abundance, reminiscent of the “ghost effect” from nonlinear dynamical systems. Integrating theory, simulations, and quantitative experiments across clonal populations and multi-species bacterial communities, we demonstrate that a transient antibiotic pulse can eliminate plasmid-free cells and create the “ghost” state that extends plasmid persistence from days to months. Our research reveals a generalizable mechanism for the prolonged ecological memory of antibiotic exposure, and underscores the need for proactive strategies to curb the spread of AMR.

Introduction

Plasmids are self-replicating genetic elements that play a critical role in bacterial evolution by enabling the acquisition, maintenance, and dissemination of adaptive traits such as antimicrobial resistance (AMR)[1-3], giving rise to many multidrug-resistant high-risk clones[4,5] and accelerating the global AMR crisis[3]. Although plasmid carriage is often assumed to be burdensome in the absence of selection, leading to rapid plasmid loss[6,7], empirical studies suggest otherwise. Resistance frequency often remains high for months after short-term antibiotic treatments (days to weeks), despite the absence of continued selective pressure thereafter[8-12]. Given that many resistance determinants reside on plasmids[11,13-19], the slow resistance reversal suggests burdensome plasmid can still experience long transients after antibiotic exposure.

Different mechanisms may account for this prolonged persistence after antibiotic treatment. For instance, positive selection can increase the frequency of compensatory mutations that reduce the cost of plasmid carriage and slow down the decay of plasmids[20]. Long half-life of certain antibiotics can exert sustained selection for resistance after the treatment ceased[9]. More broadly, the persistence or slow reversal of resistance or plasmid carriage can be associated with low or zero fitness cost[6,21-23], high conjugation rate[24-26], or both[24,27]. Co-selection by antibiotics[6,28] or environmental contaminants[29] on the same mobilizable gene elements has also been proposed. However, these mechanisms cannot account for the slow decay of plasmids whose baseline abundance is low, i.e., burdensome, slow-transferring plasmids get lost fast.

Past theories suggest another under-appreciated possibility: the slow segregation loss of plasmids[30,31]. While largely ignored due to its relatively minor contribution to plasmid steady state persistence[24,25,27], slow segregation loss can sustain plasmid carriage in clones for a long time [32,33], before plasmid-encoded high-burden cargoes drive the plasmid to get completely lost. This provides a theoretical basis for the prolonged plasmid carriage following antibiotic exposure: antibiotics can eliminate the plasmid-free competitor cells, so the plasmid needs to go through the slow segregation loss process before rapidly decrease in their abundance due to the growth competition from plasmid-free segregant.

Here, we combine theory, numerical simulations, and quantitative experiments to demonstrate this principle in clonal populations, synthetic *E. coli* communities, and multi-species communities of hospital sink isolates: the decoupling of time scales between segregation loss and growth competition can lead to the observed prolonged ecological memory of plasmids. This

principle underscores the need to develop active intervention strategies beyond standard antibiotic stewardship.

Results

Population ghost effect slows down plasmid abundance decay

We start from a simple ordinary differential equation (ODE) model depicting the dynamics of a non-mobilizable plasmid within a single strain population (**Methods**). The dynamics of plasmid loss in a population are mainly dictated by two processes: *(1) segregation loss*, where a daughter cell fails to inherit the plasmid during cell division (**Fig. 1a**, pink), and *(2) growth competition*, where plasmid-carrying cells are outcompeted by plasmid-free population due to plasmid-imposed metabolic burden on their host (**Fig. 1a**, purple). Segregation loss is generally a slow process, where different plasmids can deploy active partitioning, post-segregational killing, and high copy-number to minimize its loss during cell division[34,35]. Meanwhile, growth competition operates on a faster timescale.

We used the ODE model to simulate plasmid abundance (fraction of plasmid carrying cells in a population) over time (**Fig. 1b**), across different initial plasmid abundances of P_0% = 100%, 99%, 90%, 50%, and 20%. When starting from a pure plasmid-carrying population (P_0% = 100%), plasmid abundance decays in two phases, corresponding to the two processes: an initial slow decay driven by segregation loss, followed by a faster decay driven by growth competition once plasmid-free cells have emerged. This two-phase behavior is consistent with previous experimental observations[32,36], where the presence of post-segregational killing mechanism results in a long plateau in which plasmid abundance remains ~100%. In the absence of active partitioning or post-segregational killing mechanisms, this plateau was significantly shortened or even eliminated. As the initial plasmid abundance decreases, growth competition becomes more prominent, driving the plasmid abundance decay exponentially. Based on a previous work[30], we can analytically derive the half-life of plasmid abundance decay (**Methods**) which nonlinearly increases with initial plasmid abundance (**Fig. 1c**). When P_0% << 100%, the abundance decays exponentially with half-life $\tau_{1/2} = \frac{1}{\delta}\log 2$. When P_0% = 100%, plasmid half-life becomes $\tau_{1/2} \rightarrow \frac{1}{\delta}\log(\frac{\delta}{\kappa})$, where δ is the rate of growth competition between the plasmid-free and plasmid-carrying populations, and κ is the segregation loss rate. In most cases, $\kappa \ll \delta$ [24], thus half-life $\tau_{1/2}$ becomes large, and the high abundance state appear as the "ghost" of an equilibrium[37]. This logarithmic scaling between κ and $\tau_{1/2}$ resembles the "ghost effect" coined by Strogatz[37],

107 originally referring to the loss of stability in a dynamical system during saddle-node bifurcation.
108 The prolonged plasmid carriage in our case instead arises from the remnant of a saddle point
109 (when κ changes from 0 to a small number).
110
111 To verify our prediction of diverging half-lives near pure population, we monitored the
112 abundance of three non-mobilizable plasmids with different origin of replication, pSC101
113 (kanamycin resistant, Kan^R), colE1 (Kan^R), and pUC (spectinomycin, $Spect^R$), all encoding sfGFP,
114 in *E. coli* strain MG1655 over time (**Fig. 1d & Fig. S1**). To facilitate high-throughput measurements,
115 we used the GFP/OD ratio to quantify plasmid abundance (calibration details in **Methods**).
116 Plasmid-carrying MG1655 cells were mixed with plasmid-free MG1655 cells at different volume
117 ratios to generate populations where plasmid carrying cells make up of 100%, 99%, 90%, 50% or
118 20% of the total population. Populations were cultured in LB and diluted 1:500 every 24 hours
119 (**Methods**). As predicted by the mathematical model, a plateau in plasmid abundance was
120 observed at high initial abundances before exponential decay (**Fig. S1b**), significantly prolonging
121 the half-life of plasmid abundance. Thus, the initial purity of the community, in terms of the
122 plasmid-carrying cell population, dictates the plasmid half-life (**Fig. 1 e - g**). Interestingly, at P_0%
123 = 100%, pUC persisted in the community. As a high copy plasmid[38], the stochastic chance of pUC
124 to have segregation error becomes extremely small, preventing the birth of plasmid-free cells and
125 the subsequent growth competition. Moreover, for the populations with plasmid abundance decay
126 (pUC with P_0% = 99% and 90%, and colE1 with P_0% = 99%), the plasmid abundances sometimes
127 rebounded, suggesting potential compensatory mutations.
128
129 We further quantified the dynamics of two conjugative plasmids, pCU1 and R6K in *E. coli*
130 DA28102, with daily 100-fold dilution in LB media supplemented with 25 μg/mL chloramphenicol
131 (Cm) to prevent contamination. Both pCU1 and R6K exhibited slowed-down decays and diverging
132 half-lives when P_0% is near 100% (**Fig. 1h & i, Fig. S2**).
133
134 **Transient antibiotic selection extends plasmid half-life through purifying selection**
135 Antibiotics can eliminate plasmid-free cells in a population and purify the population to
136 enter the ghost effect region (**Fig. 2a**). We thus hypothesize selection with antibiotics could
137 prolong the carriage of a plasmid. We assembled populations of *E. coli* MG1655 with an equal
138 mixture of plasmid-free and plasmid-carrying cells (P_0%=50%). We used the non-mobilizable,
139 sfGFP-encoding plasmids pSC101, colE1, and pUC for high-throughput measurement. We
140 applied a pulse of antibiotic selection to the populations between day 2 and 3. After growing the

141 population in LB supplemented with a gradient of antibiotics (Kan for pSC101 and colE1, and
142 Spect for pUC) for 24 hours, we removed the selection and tracked the GFP/OD readout over
143 time (**Fig. 2b – d, Fig. S3b**). We found the half-lives of the three plasmids all positively correlate
144 with the dosage of antibiotic selection (**Fig. 2e - g**), and plateaus above critical concentrations.
145 The critical concentrations are 3.125 μg/mL Kan for pSC101, 6.25 μg/mL Kan for colE1, and 12.5
146 μg/mL Spect for pUC.
147
148 **Antibiotic pulse induces prolonged plasmid carriage in synthetic *E. coli* communities**
149 To determine whether the ghost effect occurs in more complex microbial systems, we
150 constructed five synthetic communities of *E. coli* Keio strains[39]. Each strain contains a uniquely
151 barcoded, non-mobilizable plasmid, enabling the quantification of community structure using next
152 generation sequencing (NGS). The first community, Comm87, consisted of 86 background strains
153 plus one donor strain carrying conjugative plasmid R388 (trimethoprim resistant, $Trim^R$). Four
154 other communities (Comm57) shared the same background community of 56 barcoded Keio
155 strains, in addition to a unique donor strain carrying one additional conjugative plasmid, either
156 R6K (streptomycin resistant, $Strp^R$), pCU1 (carbenicillin resistant, $Carb^R$), R388, and RP4
157 (tetracycline resistant, Tet^R). The overnight cultures of the background strains were equally
158 combined, then mixed with the donor strain at a 3:1 ratio to assemble each of the five communities.
159 The communities were passaged daily with a 100-fold dilution in LB media supplemented with
160 100 μg/mL Carb for Comm 87 or 25 μg/mL Cm for Comm 57 to maintain the barcode plasmids.
161 We tracked the abundance of the target plasmids over time through selective plating.
162
163 Without any additional antibiotic intervention, the conjugative plasmids exponentially
164 decayed (**Fig. 3a - c**, purple), with half-lives of 2.2 (±SD = 0.4, n=3) days for R388 in Comm87,
165 4.4 (±0.1) days for R6K in Comm57, and 1.0 (±0.1) days for pCU1 in Comm57 (**Fig. 3d - f**). R388
166 and RP4 were able to persist in Comm57 for the entire course of the 20-day xperiment (**Fig. 3g**
167 **& h**). As predicted by the model, antibiotic selection for the plasmids, applied between day 2 and
168 3, increased plasmid abundances to ~ 100%. Driving the communities into the ghost effect region
169 significantly extended plasmid half-lives to 27.3 (±1.7) days for R388 in Comm87 and 9.9 (±0.9)
170 days for pCU1 in Comm57 (**Fig. 3 d-f,** $p<0.01$ or $p<0.001$ with Welch's t-test). Plasmids R6K,
171 R388, and RP4 all persisted in the communities at ~100% for more than 17 days after antibiotic
172 selection (**Fig. 3b, g, h**, orange). The four Comm57 communities, when passaged in a different
173 dilution rate (1:500), showed similar results (**Fig. S4**).
174

We used NGS to quantify the community composition over time (**Fig. 3i & Fig. S5**). Upon antibiotic selection, a significant shift in each community structure was observed, and the community diversity dropped significantly (**Fig. S6**). Upon selection, the relative abundances of the plasmid donors were significantly amplified (**Fig. 3j**), while the donor abundances decreased in most communities without antibiotic pulse. The decline in diversity, and the increase in donor abundance, suggests that the plasmids have not yet spread to every member in the community. One exception was Comm57 harboring RP4, where the donor abundance was significantly decreased upon antibiotic selection (**Fig. 3j**). While in other communities the antibiotic pulse resulted in a crash in diversity, the RP4 community instead increased its diversity (**Fig. S6**). This could be due to the combination of two factors: the low fitness of the donor strain, and the fast conjugation capacity of RP4[24,40]. By the time positive selection takes place, most strains in the community would have already received the plasmid, and could outcompete the donor strain in the presence of Tet.

These findings demonstrate that the ghost effect operates not only in clonal populations but also in synthetic microbial communities. A brief antibiotic pulse can reorganize community composition by selectively eliminating plasmid-free competitors, thereby stabilizing plasmid persistence at the community level without requiring genetic adaptation.

Ghost effect in multi-specific communities with niche partition

In natural ecosystems, microbes can co-exist in natural communities through niche partition, where different species / strains can take up different resources (**Fig. 4a**) or habitats (**Fig. 4b**) to avoid competitive exclusion. In the above experiments, we showed the ghost effect taking place in clonal populations and *E. coli* communities, where strong competitions exist between individual strains, and thus plasmid-free and plasmid-carrying populations. In these cases, ghost effect takes place when the plasmid abundance reaches ~100%. However, numerical simulations (**Methods**) suggest antibiotic-induced ghost effect can happen without community purity (**Fig. 4 c & d**) with niche partition. For instance, consider a mixed population of plasmid-free strain 1, plasmid-carrying strain 1, and non-host strain 2 (**Methods**). In the simple case where (1) strain 1 and 2 do not interact and (2) strain 2 has moderate resistance to the antibiotic, the non-host strain 2 can survive the antibiotic selection, limiting the plasmid abundance to < 100%. However, ghost effect can still happen within the purified strain 1 population, resulting in the prolonged carriage of the plasmid in the two-member community (**Fig. 4c & d**). In essence, as long as the plasmid-carrying population is pure within a given niche, ghost effect should take

place. Since natural microbiomes often have niche partition, with different species exhibiting natural or acquired resistance, we expect general applicability of ghost effect following antibiotic treatments, even when the plasmid or resistance abundance does not reach 100%.

To demonstrate this idea, we constructed three communities consisting of 8 isolates from Duke Hospital sink p-traps[41] (**Methods**), plasmid-free and plasmid-carrying *E. coli* MG1655 with one of the three non-mobilizable plasmids (pSC101, colE1 and pUC) expressing sfGFP as a surrogate for their abundance. The sink isolates consist of one *Pseudomonas Aeruginosa* strain, three *Bacillus* trains, one *Citrobacter* strain, and three *Enterobacter* strains (**Fig. 4e**). To facilitate niche partitioning, we used cellulose sponges immersed in LB media to create porous, physically partitioned habitats (**Fig. 4e**), which were previously found to promote the diversity of microbial communities[42].

In the absence of antibiotic selection, the GFP/OD level (**Methods**) dropped rapidly to below 10^2. After transient Kan or Spect selection between day 1 and 2, GFP expression was increased. pSC101 showed slowed decay in GFP/OD level, while colE1 and pUC persisted until day 10 (**Fig. 4 f – h**). This is consistent with our observations of the three plasmids in clonal populations (**Fig. 1, Fig. S1**). Importantly, for plasmids colE1 and pUC, the GFP/OD levels were consistently below the baseline in pure plasmid-carrying MG1655 populations.

Through 16S sequencing (**Methods**), we quantified community dynamics in the presence and absence of the transient antibiotic treatment (**Fig. 4 i – k**). On day 2, in the absence of antibiotics, *P. aeruginosa* and *Enterobacter* became dominant in the communities, with the other three genera decreasing in their fractions or even become undetectable in some of the replicates. Antibiotic treatment increased the abundance of the two resistant strains, *E. coli* and *P. aeruginosa*, and eliminated the rest of the community. The survival of *P. aeruginosa* confirms that the communities do not purely contain plasmid-carrying cells, but a ghost effect within the *E. coli* population still takes place. Consistent with the GFP/OD reading of pSC101, *P. aeruginosa* was detectable in one of the three replicate communities harboring pSC101, potentially due to the stochastic effect of high dilution rate (2×10^7) during daily passaging.

In LB cultures without cellulose sponges, the GFP/OD levels of the communities after antibiotic treatment became comparable to the pure plasmid-carrying baselines (Fig. S7) and exhibited slowed-down decay in comparison to the antibiotic-free control group. Since the

243 plasmids are non-mobilizable, the post-treatment communities likely consisted primarily of *E. coli*.
244 In contrast, the survival of *P. aeruginosa* should be attributed to the presence of sponges, which
245 possibly introduces spatial structures to mediate the competition[42] and promote biofilm formation[43].
246

Discussion

Resistance limits the clinical efficacy of antibiotic treatments and poses a major threat to human health. Many antibiotic resistance genes are maintained and propagated by mobile genetic elements including plasmids[1-3]. Understanding and predicting the persistence of plasmids is critical for designing intervention strategies to contain and reverse the spread of AMR. In this work, we systematically quantified the decay dynamics of multiple plasmids across different community contexts, and established their dependence on community structure. We showed that the plasmid half-life diverges in nearly pure plasmid-carrying populations, either from assembly or induced by transient antibiotic pulse, extending the plasmid's survival for months. Theoretically, this ghost effect arises from the decrease in the strength of growth competition when plasmid-free cells are scarce in the population.

Our results reveal a common mechanism underlying slow reversal of plasmid-mediated resistance after antibiotic treatments, a phenomenon that spans across microbial ecosystems ranging from the human oral, urinary, and gut microbiomes, to those of livestock. Macrolide antibiotics have been reported to increase the abundance of resistant streptococci (primarily carrying *mef* gene or macrolide-lincosamide-streptogramin-B resistant cassette *erm*(B)) in oral microbiomes to more than 80%, which requiring over 6 months to revert to baseline[9]. The authors attributed this prolonged resistance carriage to the long half-life of azithromycin, and the low burden of the *erm*(B) gene. Similarly, veterinary β-lactams strongly amplified the abundance of resistant bacteria in the pig intestinal microbiome, persisting for more than 3 weeks beyond the drug withdrawal. The extended-spectrum β-lactamase CTX-M-1 was carried by both an exogenous conjugative plasmid and indigenous gut microbiota. Consistent with our results (**Fig. 3, Fig. S5**), the authors observed the significant amplification of resistance abundance and donor abundance upon antibiotic selection, followed by rapid decline of the donor strain abundance after antibiotic withdrawal. Importantly, both the *erm*(B) cassette [13-17] and the CTX-M-1 gene[18,19] are commonly found on conjugative plasmids and other mobilizable gene elements. Yelin et al. reported that resistance in urinary tract infections shows autocorrelation lasting more than six months, with strong and persistent correlation between patients' antibiotic purchase history and subsequent resistance[12]. Anthony et al. observed increases in the abundance of β-lactam, macrolide, and tetracycline resistance following treatment with cephalosporin (β-lactam), azithromycin (macrolide), or both[10]. During the development of the infant gut microbiome, resistance genes on mobile genetic elements were found to persist longer than those encoded on chromosomes[11]. The diversity of antibiotics, resistance genes, bacterial host, and ecosystems

281 all point to a general population-dynamical mechanism. As the ghost effect depends only on the
282 slow time scale of segregation loss, it provides a generalizable theoretical framework for these
283 observed phenomena. Consequently, persistent resistance has important implications for clinical
284 practice and food production, as it provides a reservoir for the community spread of AMR.
285
286 While our work focuses on the population dynamics of the plasmids, the ghost effect also
287 has strong evolutionary consequences. Prolonged plasmid carriage enables co-evolution of the
288 plasmid and host, creating opportunities for compensatory mutations. Long-term co-evolution
289 could ameliorate the burden of the plasmid[20], and may even turn the deleterious cost of plasmid
290 carriage to a beneficial one[22]. Thus, despite predictions that certain plasmids should not persist
291 based on ecological models[24,27], their long-term persistence may occur before eventual extinction.
292 In our experiments, we observed potential evolutionary rescues for colE1 and pUC starting at high
293 initial plasmid abundances (**Fig. S1**), which was not observed in populations outside of the ghost
294 effect region. Therefore, plasmid persistence can have bistable outcomes when evolution forces
295 are taken into consideration.
296
297 The antibiotic-induced persistence also provides an environment-driven explanation for
298 the survival of burdensome plasmids, addressing the so-called plasmid paradox[7]. Previous
299 studies have attributed plasmid survival to biotic factors, such as fast conjugation[24,25,44], variable
300 fitness effects across different hosts[23], spatial partitioning[45], and compensatory mutations that
301 ameliorates the plasmid burden[20,22]. These works typically assume constant environments,
302 without positive selections on the plasmids. However, plasmids in natural and clinical settings
303 experience fluctuating selection forces[46-50]. In such cases, the burdensome plasmids can persist
304 when the frequency of positive selection is on the same order of magnitude as the plasmid half-
305 life within the ghost effect region. This mechanism further raises questions about the efficacy of
306 simply reducing antibiotic use to contain AMR[6] – similar persistence can be achieved with far less
307 amount of antibiotics with sporadic selection. Conversely, pulsed antibiotic treatments has been
308 proposed as a strategy to constrain the development of resistance[51-55]. Such strategies should
309 avoid the ghost effect region in design to prevent slow population responses that disproportionally
310 favor resistant bacteria.
311
312 The clinical, ecological, and evolutionary implications of ghost effect underscore the need
313 for strategies that counteract against unintended antibiotic exposure. Previous studies have used
314 chemicals to reduce plasmid abundance and reverse its persistence[24,56]. As both plasmid

315 abundance and half-life are governed by conjugation, growth, and segregation events[27], we
316 hypothesize that these chemicals could also accelerate plasmid decay. We found that curing
317 chemicals and their combinations were able to reduce the half-life of pSC101 almost by half (**Fig.**
318 **S8**). A single day of treatment using chemical combinations achieved comparable effects as full
319 course, suggesting these chemicals may accelerate the plasmid decay by increasing segregation
320 error.
321
322 Overall, our work established the timescale decoupling between segregation loss and
323 growth competition for burdensome plasmids, and demonstrated the disproportionate impact of
324 transient antibiotic pulses on the plasmid persistence. Our findings provide a generalizable
325 mechanism for the prolonged ecological memory of plasmid carriage following antibiotic exposure,
326 and have implications for clinical management of antibiotic use and the ecology and evolution of
327 plasmids.
328

Acknowledgments

We thank Emma Chory, Teng Wang, Rohan Maddemsetti, Emrah Şimşek, Grayson Hamrick, Yifan Dai, and Aaron Yip for helpful discussions. This work was supported by National Institute of Health (L.Y.: R01AI125604, R01GM098642, R01EB031869) and the National Science Foundation (L. Y.: Cooperative Agreement No. EEC-2133504)

Author contributions

Z.Z., A.W., and L.Y. conceived the research. Z.Z., A.W., Z.Y., X.C., and K.L. performed the experiments. Z.Z. performed the modelling and statistical analysis. Z.Z., A.W., and L.Y. wrote the manuscript. All authors read and contributed to the manuscript.

Declaration of interests

The authors declare no competing interests.

Declaration of generative AI and AI-assisted technologies in the writing process

During the preparation of this work the authors used ChatGPT to improve the language of the manuscript. After using this tool, the authors reviewed and edited the content as needed and take full responsibility for the content of the published article.

Resource availability

Materials availability

Genetic constructs generated for this study are available upon request.

Lead contact

Further information and requests for resources should be directed to and will be fulfilled by the lead contact, Lingchong You (you@duke.edu).

Data and code availability

All original code and data have been deposited at https://github.com/youlab/Plasmid-Ghost-Effect.

361 **References**

362 1 Bethke, J. H. *et al.* Environmental and genetic determinants of plasmid mobility in pathogenic
363 Escherichia coli. *Science Advances* **6**, eaax3173 (2020).
364 https://doi.org:10.1126/sciadv.aax3173
365 2 Lipworth, S. *et al.* The plasmidome associated with Gram-negative bloodstream infections: A
366 large-scale observational study using complete plasmid assemblies. *Nature Communications* **15**
367 (2024). https://doi.org:10.1038/s41467-024-45761-7
368 3 Castañeda-Barba, S., Top, E. M. & Stalder, T. Plasmids, a molecular cornerstone of antimicrobial
369 resistance in the One Health era. *Nature Reviews Microbiology* **22**, 18-32 (2024).
370 https://doi.org:10.1038/s41579-023-00926-x
371 4 Hawkey, P. M. & Jones, A. M. The changing epidemiology of resistance. *J Antimicrob Chemother*
372 **64 Suppl 1**, i3-10 (2009). https://doi.org:10.1093/jac/dkp256
373 5 Mathers, A. J., Peirano, G. & Pitout, J. D. The role of epidemic resistance plasmids and
374 international high-risk clones in the spread of multidrug-resistant Enterobacteriaceae. *Clin*
375 *Microbiol Rev* **28**, 565-591 (2015). https://doi.org:10.1128/cmr.00116-14
376 6 Andersson, D. I. & Hughes, D. Antibiotic resistance and its cost: is it possible to reverse
377 resistance? *Nature Reviews Microbiology* **8**, 260-271 (2010).
378 https://doi.org:10.1038/nrmicro2319
379 7 Brockhurst, M. A. & Harrison, E. Ecological and evolutionary solutions to the plasmid paradox.
380 *Trends in Microbiology* **30**, 534-543 (2022). https://doi.org:10.1016/j.tim.2021.11.001
381 8 Cavaco, L. M., Abatih, E., Aarestrup, F. M. & Guardabassi, L. Selection and persistence of CTX-M-
382 producing Escherichia coli in the intestinal flora of pigs treated with amoxicillin, ceftiofur, or
383 cefquinome. *Antimicrob Agents Chemother* **52**, 3612-3616 (2008).
384 https://doi.org:10.1128/aac.00354-08
385 9 Malhotra-Kumar, S., Lammens, C., Coenen, S., Van Herck, K. & Goossens, H. Effect of
386 azithromycin and clarithromycin therapy on pharyngeal carriage of macrolide-resistant
387 streptococci in healthy volunteers: a randomised, double-blind, placebo-controlled study. *The*
388 *Lancet* **369**, 482-490 (2007). https://doi.org:10.1016/S0140-6736(07)60235-9
389 10 Anthony, W. E. *et al.* Acute and persistent effects of commonly used antibiotics on the gut
390 microbiome and resistome in healthy adults. *Cell Reports* **39**, 110649 (2022).
391 https://doi.org:10.1016/j.celrep.2022.110649
392 11 Yassour, M. *et al.* Natural history of the infant gut microbiome and impact of antibiotic
393 treatment on bacterial strain diversity and stability. *Sci Transl Med* **8**, 343ra381 (2016).
394 https://doi.org:10.1126/scitranslmed.aad0917
395 12 Yelin, I. *et al.* Personal clinical history predicts antibiotic resistance of urinary tract infections.
396 *Nature Medicine* **25**, 1143-1152 (2019). https://doi.org:10.1038/s41591-019-0503-6
397 13 Berryman, D. I. & Rood, J. I. The closely related ermB-ermAM genes from Clostridium
398 perfringens, Enterococcus faecalis (pAM beta 1), and Streptococcus agalactiae (pIP501) are
399 flanked by variants of a directly repeated sequence. *Antimicrob Agents Chemother* **39**, 1830-
400 1834 (1995). https://doi.org:10.1128/aac.39.8.1830
401 14 Clewell, D. B., Flannagan, S. E. & Jaworski, D. D. Unconstrained bacterial promiscuity: the Tn916-
402 Tn1545 family of conjugative transposons. *Trends Microbiol* **3**, 229-236 (1995).
403 https://doi.org:10.1016/s0966-842x(00)88930-1
404 15 Horodniceanu, T., Bouanchaud, D. H., Bieth, G. & Chabbert, Y. A. R plasmids in Streptococcus
405 agalactiae (group B). *Antimicrob Agents Chemother* **10**, 795-801 (1976).
406 https://doi.org:10.1128/aac.10.5.795

16 Leblanc, D. J. & Lee, L. N. Physical and genetic analyses of streptococcal plasmid pAM beta 1 and cloning of its replication region. *Journal of Bacteriology* **157**, 445-453 (1984). https://doi.org:10.1128/jb.157.2.445-453.1984

17 Shaw, J. H. & Clewell, D. B. Complete nucleotide sequence of macrolide-lincosamide-streptogramin B-resistance transposon Tn917 in Streptococcus faecalis. *J Bacteriol* **164**, 782-796 (1985). https://doi.org:10.1128/jb.164.2.782-796.1985

18 Cormier, A. C. *et al.* Diversity of blaCTX-M-1-carrying plasmids recovered from Escherichia coli isolated from Canadian domestic animals. *PLOS ONE* **17**, e0264439 (2022). https://doi.org:10.1371/journal.pone.0264439

19 Dolejska, M., Villa, L., Hasman, H., Hansen, L. & Carattoli, A. Characterization of IncN plasmids carrying bla CTX-M-1 and qnr genes in Escherichia coli and Salmonella from animals, the environment and humans. *J Antimicrob Chemother* **68**, 333-339 (2013). https://doi.org:10.1093/jac/dks387

20 San Millan, A. *et al.* Positive selection and compensatory adaptation interact to stabilize non-transmissible plasmids. *Nature Communications* **5**, 5208 (2014). https://doi.org:10.1038/ncomms6208

21 Enne, V. I. *et al.* Assessment of the fitness impacts on Escherichia coli of acquisition of antibiotic resistance genes encoded by different types of genetic element. *Journal of Antimicrobial Chemotherapy* **56**, 544-551 (2005). https://doi.org:10.1093/jac/dki255

22 Loftie-Eaton, W. *et al.* Compensatory mutations improve general permissiveness to antibiotic resistance plasmids. *Nature Ecology & Evolution* **1**, 1354-1363 (2017). https://doi.org:10.1038/s41559-017-0243-2

23 Alonso-del Valle, A. *et al.* Variability of plasmid fitness effects contributes to plasmid persistence in bacterial communities. *Nature Communications* **12**, 2653 (2021). https://doi.org:10.1038/s41467-021-22849-y

24 Lopatkin, A. J. *et al.* Persistence and reversal of plasmid-mediated antibiotic resistance. *Nature Communications* **8** (2017). https://doi.org:10.1038/s41467-017-01532-1

25 Hall, J. P. J., Wood, A. J., Harrison, E. & Brockhurst, M. A. Source–sink plasmid transfer dynamics maintain gene mobility in soil bacterial communities. *Proceedings of the National Academy of Sciences* **113**, 8260-8265 (2016). https://doi.org:10.1073/pnas.1600974113

26 Alonso-Del Valle, A. *et al.* Antimicrobial resistance level and conjugation permissiveness shape plasmid distribution in clinical enterobacteria. *Proceedings of the National Academy of Sciences* **120** (2023). https://doi.org:10.1073/pnas.2314135120

27 Wang, T. & You, L. The persistence potential of transferable plasmids. *Nature Communications* **11** (2020). https://doi.org:10.1038/s41467-020-19368-7

28 Wang, X. *et al.* Inter-plasmid transfer of antibiotic resistance genes accelerates antibiotic resistance in bacterial pathogens. *Isme j* **18** (2024). https://doi.org:10.1093/ismejo/wrad032

29 Murray, L. M. *et al.* Co-selection for antibiotic resistance by environmental contaminants. *npj Antimicrobials and Resistance* **2**, 9 (2024). https://doi.org:10.1038/s44259-024-00026-7

30 Cooper, N. S., Brown, M. E. & Caulcott, C. A. A Mathematical Method for Analysing Plasmid Stability in Micro-organisms. *Microbiology* **133**, 1871-1880 (1987). https://doi.org:10.1099/00221287-133-7-1871

31 Summers, D. K. The kinetics of plasmid loss. *Trends in Biotechnology* **9**, 273-278 (1991). https://doi.org:https://doi.org/10.1016/0167-7799(91)90089-Z

32 Fedorec, A. J. H. *et al.* Two New Plasmid Post-segregational Killing Mechanisms for the Implementation of Synthetic Gene Networks in Escherichia coli. *iScience* **14**, 323-334 (2019). https://doi.org:10.1016/j.isci.2019.03.019

33 Danino, T. *et al.* Programmable probiotics for detection of cancer in urine. *Science Translational Medicine* **7**, 289ra284-289ra284 (2015). https://doi.org:10.1126/scitranslmed.aaa3519

34 Nordström, K. & Austin, S. J. MECHANISMS THAT CONTRIBUTE TO THE STABLE SEGREGATION OF PLASMIDS. *Annual Review of Genetics* **23**, 37-69 (1989). https://doi.org:https://doi.org/10.1146/annurev.ge.23.120189.000345

35 Baxter, J. C. & Funnell, B. E. Plasmid Partition Mechanisms. *Microbiol Spectr* **2** (2014). https://doi.org:10.1128/microbiolspec.PLAS-0023-2014

36 Cooper, T. F. & Heinemann, J. A. Postsegregational killing does not increase plasmid stability but acts to mediate the exclusion of competing plasmids. *Proceedings of the National Academy of Sciences* **97**, 12643-12648 (2000). https://doi.org:10.1073/pnas.220077897

37 Strogatz, S. a. *Nonlinear dynamics and chaos : with applications to physics, biology, chemistry, and engineering*. (Second edition. Boulder, CO : Westview Press, a member of the Perseus Books Group, [2015], 2015).

38 Shao, B. *et al.* Single-cell measurement of plasmid copy number and promoter activity. *Nature Communications* **12**, 1475 (2021). https://doi.org:10.1038/s41467-021-21734-y

39 Baba, T. *et al.* Construction of Escherichia coli K-12 in-frame, single-gene knockout mutants: the Keio collection. *Mol Syst Biol* **2**, 2006.0008 (2006). https://doi.org:10.1038/msb4100050

40 Wang, T. *et al.* Horizontal gene transfer enables programmable gene stability in synthetic microbiota. *Nature Chemical Biology* (2022). https://doi.org:10.1038/s41589-022-01114-3

41 Şimşek, E. *et al.* Keystone engineering enables collective range expansion in microbial communities. *bioRxiv*, 2025.2001.2011.632568 (2025). https://doi.org:10.1101/2025.01.11.632568

42 Wu, F. *et al.* Modulation of microbial community dynamics by spatial partitioning. *Nature Chemical Biology* **18**, 394-402 (2022). https://doi.org:10.1038/s41589-021-00961-w

43 Agustín, M. D., Stengel, P., Kellermeier, M., Tücking, K.-S. & Müller, M. Monitoring Growth and Removal of Pseudomonas Biofilms on Cellulose-Based Fabrics. *Microorganisms* **11** (2023).

44 Stevenson, C., Hall, J. P. J., Harrison, E., Wood, A. J. & Brockhurst, M. A. Gene mobility promotes the spread of resistance in bacterial populations. *The ISME Journal* **11**, 1930-1932 (2017). https://doi.org:10.1038/ismej.2017.42

45 Weiss, A., Wang, T. & You, L. Promotion of plasmid maintenance by heterogeneous partitioning of microbial communities. *Cell Systems* **14**, 895-905.e895 (2023). https://doi.org:10.1016/j.cels.2023.09.002

46 Stevenson, C., Hall, J. P. J., Brockhurst, M. A. & Harrison, E. Plasmid stability is enhanced by higher-frequency pulses of positive selection. *Proceedings of the Royal Society B: Biological Sciences* **285**, 20172497 (2018). https://doi.org:10.1098/rspb.2017.2497

47 Cai, M. *et al.* Occurrence and temporal variation of antibiotics and antibiotic resistance genes in hospital inpatient department wastewater: Impacts of daily schedule of inpatients and wastewater treatment process. *Chemosphere* **292**, 133405 (2022). https://doi.org:https://doi.org/10.1016/j.chemosphere.2021.133405

48 Cao, S., Zhang, P., Halsall, C., Hou, Z. & Ge, L. Occurrence and seasonal variations of antibiotic micro-pollutants in the Wei River, China. *Environmental Research* **252**, 118863 (2024). https://doi.org:https://doi.org/10.1016/j.envres.2024.118863

49 Schuster, D. *et al.* Antibiotic concentrations in raw hospital wastewater surpass minimal selective and minimum inhibitory concentrations of resistant Acinetobacter baylyi strains. *Environ Microbiol* **24**, 5721-5733 (2022). https://doi.org:10.1111/1462-2920.16206

50 Coutu, S., Rossi, L., Barry, D. A., Rudaz, S. & Vernaz, N. Temporal Variability of Antibiotics Fluxes in Wastewater and Contribution from Hospitals. *PLOS ONE* **8**, e53592 (2013). https://doi.org:10.1371/journal.pone.0053592

502 51 Baker, C. M., Ferrari, M. J. & Shea, K. Beyond dose: Pulsed antibiotic treatment schedules can
503 maintain individual benefit while reducing resistance. *Scientific Reports* **8**, 5866 (2018).
504 https://doi.org:10.1038/s41598-018-24006-w
505 52 Letten, A. D., Hall, A. R. & Levine, J. M. Using ecological coexistence theory to understand
506 antibiotic resistance and microbial competition. *Nature Ecology & Evolution* **5**, 431-441 (2021).
507 https://doi.org:10.1038/s41559-020-01385-w
508 53 Bauer, M., Graf, I. R., Ngampruetikorn, V., Stephens, G. J. & Frey, E. Exploiting ecology in drug
509 pulse sequences in favour of population reduction. *PLOS Computational Biology* **13**, e1005747
510 (2017). https://doi.org:10.1371/journal.pcbi.1005747
511 54 Lin, W.-H. & Kussell, E. Complex Interplay of Physiology and Selection in the Emergence of
512 Antibiotic Resistance. *Current Biology* **26**, 1486-1493 (2016).
513 https://doi.org:10.1016/j.cub.2016.04.015
514 55 Nev, O. A., Jepson, A., Beardmore, R. E. & Gudelj, I. Predicting community dynamics of
515 antibiotic-sensitive and -resistant species in fluctuating environments. *Journal of The Royal*
516 *Society Interface* **17**, 20190776 (2020). https://doi.org:10.1098/rsif.2019.0776
517 56 Buckner, M. M. C., Ciusa, M. L. & Piddock, L. J. V. Strategies to combat antimicrobial resistance:
518 anti-plasmid and plasmid curing. *FEMS Microbiology Reviews* **42**, 781-804 (2018).
519 https://doi.org:10.1093/femsre/fuy031
520
521

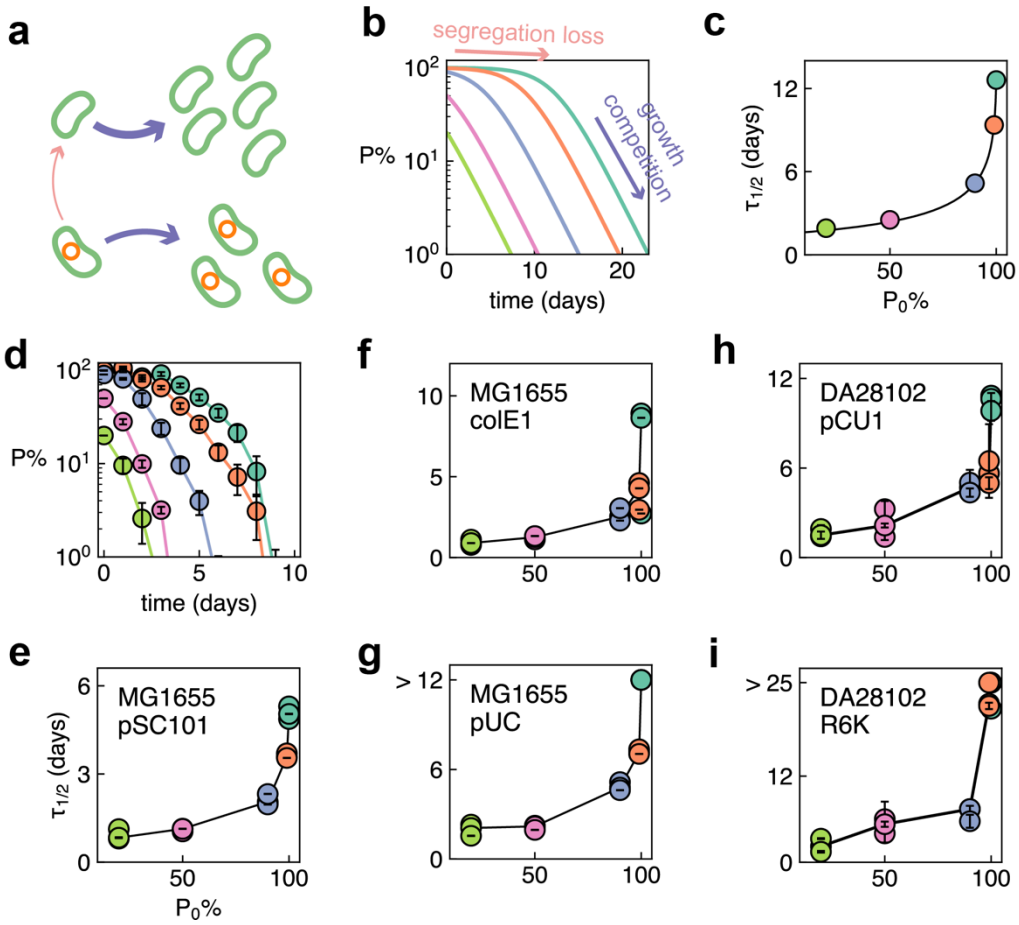

522

523 **Figure 1. High plasmid abundance nonlinearly increases plasmid half-lives.**

524 **(a).** Plasmid abundance decreases through two processes operating on different time

525 scales, slow segregation loss of the plasmid (pink) and rapid out-competition of plasmid-

526 carrying cells by plasmid-free cells (purple).

527 **(b).** Simulated time series of plasmid abundance decay. When starting from high initial

528 abundance P_0% (teal: 100%, orange: 99%), plasmid abundance exhibits biphasic

529 decay, with the slow phase driven by segregation loss (pink arrow) followed a faster

530 phase driven by growth competition (purple arrow) later. When starting from lower P_0%

531 values (dusty blue: 90%, pink: 50%, and lime green: 20%), the plasmid abundance

532 follows exponential decay.

533 **(c).** Dependence of plasmid half-life $\tau_{1/2}$ on the initial abundance P_0%. The scatter

534 points represent simulation results; the curve shows the best fit to Eq. (1) in **Methods**.

535 **(d).** Time series of pSC101 plasmid abundance decay (mean ± SE, n = 3) in *E. coli*
536 MG1655 across different P_0% (teal: 100%, orange: 99%, dusty blue: 90%, pink: 50%,
537 and lime green: 20%).
538 **(e - g).** Dependence of plasmid half-life $\tau_{1/2}$ on the initial abundance P_0% for non-
539 mobilizable plasmids **(e)** pSC101, **(f)** colE1, and **(g)** pUC. Curves connect the median
540 half-lives at each given initial abundance P_0%. Error bars indicate propagated
541 measurement uncertainties (per-well SD, delta-method in log space). Right-censored
542 datapoints ($\tau_{1/2}$ > 12 days) are shown without error bar.
543 **(h & i).** Dependence of plasmid half-life $\tau_{1/2}$ (mean ± SE based on technical triplicates
544 of selective plating) on the initial abundance P_0% for conjugative plasmids **(h)** pCU1 and
545 **(i)** R6K. Curves connect the median half-lives at each initial abundance P_0%. Right-
546 censored datapoints ($\tau_{1/2}$ > 25 days) are shown without error bar.
547

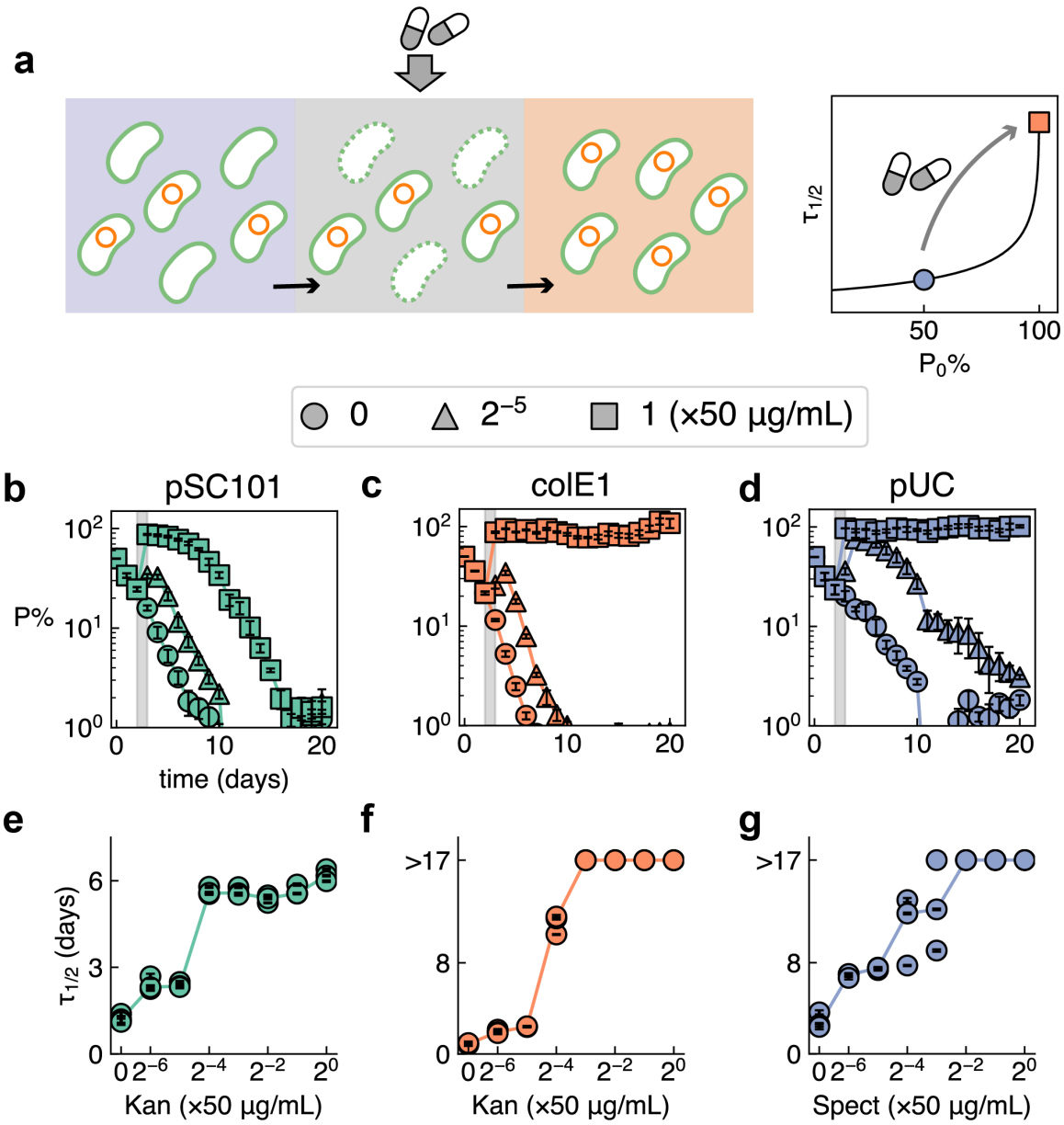

Figure 2. A transient antibiotic pulse prolongs plasmid persistence by inducing ghost effect.

(a). In a mixed population containing both plasmid-carrying and plasmid-free cells (purple), an antibiotic purifies the population by eliminating the plasmid-free cells, moving the population into the ghost effect region (orange), and extending the half-life of plasmid decay (right).

(b – d). Time series of plasmid abundance (mean ± SE, n = 3) for non-mobilizable plasmids **(b)** pSC101, **(c)** colE1, and **(d)** pUC. Between day 2 and 3 (grey), antibiotics were applied at different concentrations to induce varying levels of ghost effect. Three

558 representative conditions are shown here, corresponding to no antibiotic treatment
559 (circle), 1/32 × 50 μg/mL (triangle), and 50 μg/mL (square). pSC101 and colE1
560 populations were treated with Kan, and pUC populations were treated with Spect.
561 **(e – g).** Dose-dependence of plasmid half-lives $\tau_{1/2}$ on the pulsed antibiotic
562 concentration for **(e)** pSC101, **(f)** colE1, and **(g)** pUC. Error bars indicate propagated
563 measurement uncertainties (per-well SD, delta-method in log space). Right-censored
564 datapoints ($\tau_{1/2}$ > 17 days) are shown without error bar.
565

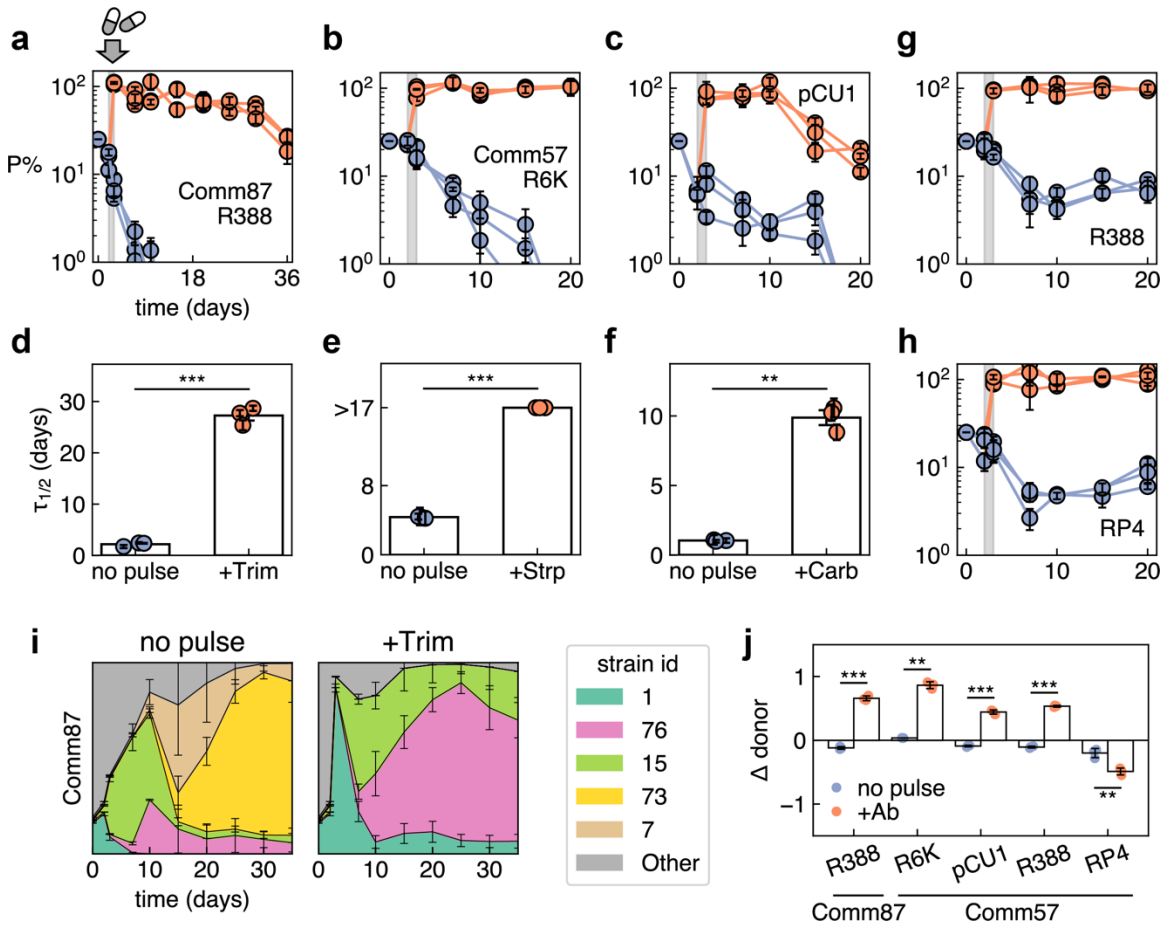

566

567 **Figure 3. Antibiotic pulse induces prolonged plasmid carriage in synthetic *E. coli***
568 **communities.**

569 **(a – c).** Plasmid abundance (mean ± SE based on technical triplicates of selective
570 plating) over time for **(a)** R388 in Comm87, **(b)** R6K in Comm60, **(c)** pCU1 in Comm 60.
571 Purple curves: communities were passaged daily at 1:100 dilution ratio in LB
572 supplemented with 100 µg/mL Carbenicillin (Comm87, **a**) or 25µg/mL Chloramphenicol
573 (Comm60, **b & c**). Orange curves: communities were treated with an additional
574 antibiotic pulse between day 2 and 3 (grey bar) to select for the plasmid-carrying
575 populations (R388: 10 µg/mL Trimethoprim, R6K: 100 µg/mL Streptomycin, pCU1: 100
576 µg/mL Carbenicillin,).

577 **(d - f)**. Antibiotic pulses extended plasmid half-lives (mean ± SE) for **(d)** R388 in
578 Comm87, **(e)** R6K in Comm60, **(f)** pCU1 in Comm 60. Right-censored datapoints ($\tau_{1/2}$ >
579 17 days) are shown without error bar. For hypothesis testing, half-lives for R6K in the
580 pulsed group (+Strp) were taken as $\tau_{1/2}$ = 17 days. **(d)** R388 half-life after Trim

581 treatment was significantly higher than in LB group: 27.3 ± 1.7 (SD) vs 2.2 ± 0.4 (SD)
582 days. Welch's t-test: t(2.21) = 24.91, p<0.001, mean difference = 25.1 [95% CI: 21.1,
583 29.1], Cohen's d = 20.34. **(e)** R6K half-life after Trim treatment was significantly higher
584 than in LB group: 17.0 ± 0.0 (SD) vs 4.4 ± 0.1 (SD) days. Welch's t-test: t(2.00) =
585 190.56, p<0.001, mean difference = 12.6 [95% CI: 12.4, 12.9], Cohen's d = 155.59. **(f)**
586 pCU1 half-life after Trim treatment was significantly higher than in LB group: 9.9 ± 0.9
587 (SD) vs 1.0 ± 0.1 (SD) days. Welch's t-test: t(2.01) = 16.50, p=0.004, mean difference =
588 8.8 [95% CI: 6.5, 11.1], Cohen's d = 13.47. In the figures, **: p < 0.01, ***: p < 0.001.
589 **(g & h).** Plasmid abundance (mean ± SE) over time for **(g)** R388 and **(h)** RP4 in
590 Comm60. Antibiotic pulsing induced alternative steady state for plasmid persistence.
591 Purple curves: communities passaged daily at 1:100 dilution ratio in LB supplemented
592 with 25μg/mL Chloramphenicol. Orange: communities were treated with additional
593 antibiotic pulse between Day 2 and 3 (grey bar) to select for the plasmid-carrying
594 populations (R388: 10 μg/mL Trimethoprim, RP4: 10 μg/mL Tetracycline).
595 **(i)**. Strain-level community dynamics (mean ± SE) of Comm87 without (left) or with
596 (right) 1-day of Trimethoprim treatment. The five most abundant strains (based on
597 cumulative relative abundance across samples) are color-coded. Strain 1 corresponds
598 to the donor strain carrying plasmid R388.
599 **(j)**. Change in the relative abundance of the donor strain (Δ donor) before (day 2) and
600 after (day 3) the antibiotic pulse. Bars represent mean ± SE (n = 3). Welch's t-test, **: p
601 < 0.01, ***: p < 0.001.
602

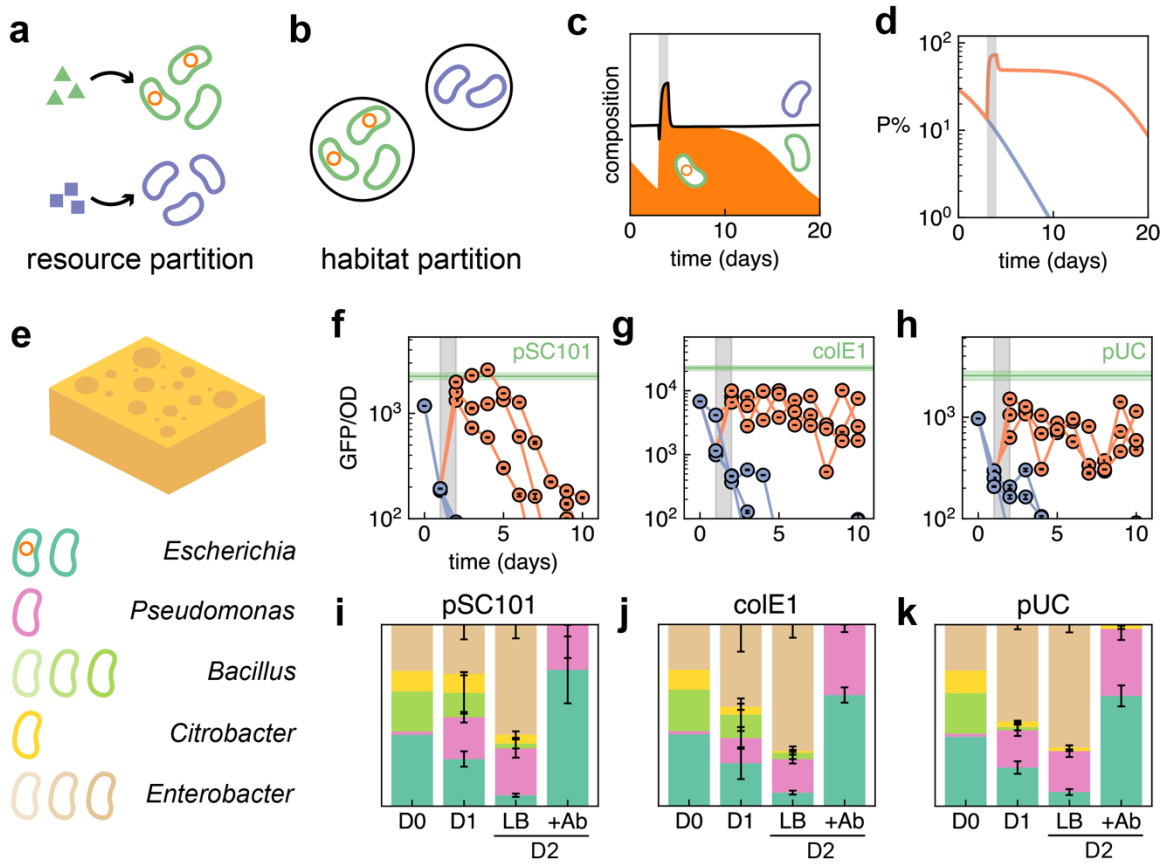

Figure 4. Ghost effect in niche partitioned communities.

(a & b). Microbes co-exist through partitioning of resource or habitat.

(c). Change in the community composition over time for a mixed population of two strains (green and purple) with complete niche partitioning (no interaction). Orange shading indicates the plasmid-carrying fraction of strain 1 (green). The community experienced selection for the plasmid-carrying cells between day 2 and 3 (gray bar).

(d). Plasmid abundance over time with (orange) and without (purple) 1-day antibiotic selection (gray bar) for the plasmid. The ghost effect occurs without plasmid abundance reaching P% = 100%.

(e). Microbial communities containing plasmid-free and plasmid-carrying *E. coli* MG1655 and eight sink isolates were cultured in LB media with sponge-imposed structure. Genus-level taxonomies of the eight sink isolates are shown. The isolates include one *Pseudomonas* strain (*P. Aeruginosa*), three *Bacillus* strains, one *Citrobacter* strain, and three *Enterobacter* strains (including one strain identified as *E. cloacae*). Strains are

618 color-coded by genus correspondingly as in (**i – k**). Three plasmids (pSC101, colE1,
619 and pUC) were separately cultured in three independent communities.
620 **(f – h).** Time series of GFP/OD for GFP-encoding plasmids pSC101, colE1, and pUC.
621 Purple: communities were passaged daily at 1:2×10^7 dilution ratio in sponges immersed
622 in LB. Orange: communities were treated with additional antibiotic pulse between day 1
623 and 2 (grey bar) to select for the plasmid-carrying populations (pSC101 and colE1: 50
624 µg/mL Kanamycin, pUC: 50 µg/mL Spectinomycin). Green bar: mean ± SE GFP/OD for
625 *E. coli* MG1655 carrying the corresponding plasmid (n = 3). Error bars indicate
626 propagated measurement uncertainties (per-well SD).
627 **(i – k).** 16S-resolved community dynamics between day 0 (D0) and day 2 (D2) (n = 1 for
628 day 0, mean ± SE, n = 3 for other samples). After the antibiotic pulse, the communities
629 were dominated by *E. coli* and *P. aeruginosa*. Due to limited taxonomic resolution of
630 16S sequencing, *E. coli* was assigned as *Escherichia-Shigella*, here we denote it as
631 *Escherichia*. Taxa with maximum relative abundance < 1% across all samples are not
632 shown.
633
634